
Exact Fractional Inference via Re-Parametrization & Interpolation between Tree-Re-Weighted- and Belief Propagation- Algorithms

Hamidreza Behjoo¹ Michael Chertkov¹

Abstract

Inference efforts – required to compute partition function, Z , of an Ising model over a graph of N “spins” – are most likely exponential in N . Efficient variational methods, such as Belief Propagation (BP) and Tree Re-Weighted (TRW) algorithms, compute Z approximately minimizing respective (BP- or TRW-) free energy. We generalize the variational scheme building a λ - fractional-homotopy, $Z^{(\lambda)}$, where $\lambda = 0$ and $\lambda = 1$ correspond to TRW- and BP-approximations, respectively, and $Z^{(\lambda)}$ decreases with λ monotonically. Moreover, this fractional scheme guarantees that in the attractive (ferromagnetic) case $Z^{(TRW)} \geq Z^{(\lambda)} \geq Z^{(BP)}$, and there exists a unique (“exact”) λ_* such that, $Z = Z^{(\lambda_*)}$. Generalizing the re-parametrization approach of (Wainwright et al., 2001) and the loop series approach of (Chertkov & Chernyak, 2006a), we show how to express Z as a product, $\forall \lambda : Z = Z^{(\lambda)} \mathcal{Z}^{(\lambda)}$, where the multiplicative correction, $\mathcal{Z}^{(\lambda)}$, is an expectation over a node-independent probability distribution built from node-wise fractional marginals. Our theoretical analysis is complemented by extensive experiments with models from Ising ensembles over planar and random graphs of medium- and large- sizes. The empirical study yields a number of interesting observations, such as (a) ability to estimate $\mathcal{Z}^{(\lambda)}$ with $O(N^4)$ fractional samples; (b) suppression of λ_* fluctuations with increase in N for instances from a particular random Ising ensemble.

1. Introduction

Graphical Models (GM) is a major tool of Machine Learning which allows to express complex statistical correlations via graphs. Ising models are most wide-spread GM expressing correlation between binary variables associated with nodes of a graph where probability is factorized into a product of terms each associated with an undirected edge of the graph. Many methods of inference and learning in GM are, first, tested on Ising models and then generalized, e.g. beyond binary and pair-wise assumptions.

In this manuscript we focus on the most difficult inference problem – computing the normalization factor, Z , – called partition function – over the Ising models. The problem is known to be of the sharp-P complexity, that is likely requiring computational efforts which are exponential in the size (number of nodes, N) of the graph (Welsh, 1991; Jerrum & Sinclair, 1993). There are three general approximate methods to compute Z : (a) elimination of (summation over) the variables one-by-one (Dechter, 1999; Dechter & Rish, 2003; Liu & Ihler, 2011; Ahn et al., 2018); (b) variational approach (Yedidia et al., 2001; 2005); (c) Monte Carlo (MS) sampling (Andrieu et al., 2003). (See also reviews (Wainwright & Jordan, 2007; Chertkov, 2023) and references there in.) In this manuscript we develop the last two of the methods. We also pay a special attention to providing and tightening approximation guarantees. We build our novel theory and algorithm on the provable upper bound for Z associated with the so-called Tree Re-Weighted (TRW) variational approximation (Wainwright, 2002; Wainwright et al., 2003; 2005) and also on the Belief Propagation (BP) variational approximation (Yedidia et al., 2001; 2005) which is known to provide low bound on Z in the case of attractive (ferromagnetic) Ising model (Rozzi, 2012).

1.1. Relation to Prior Work

In addition to the aforementioned relations to foundational work on the variational approaches (Yedidia et al., 2001; 2005), MCMC approaches (Andrieu et al., 2003), and lower and upper variational bounds (Rozzi, 2012; Wainwright et al., 2003), this manuscript also builds on recent results in other related areas, in particular:

¹Program in Applied Mathematics & Department of Mathematics, University of Arizona, Tucson, AZ. Correspondence to: Hamidreza Behjoo <hbehjoo@math.arizona.edu>, Michael Chertkov <chertkov@arizona.edu>.

- We extend the ideas of parameterized homotopy, interpolating between BP (Yedidia et al., 2001; 2005) and TRW (Wainwright, 2002; Wainwright et al., 2003; 2005), in the spirit of the fractional BP (Wiegerinck & Heskes, 2002; Chertkov & Yedidia, 2013), and therefore introducing a broader family of variational approximations.
- We utilize and generalize re-parametrization (Wainwright et al., 2001), gauge transformation and loop calculus (Chertkov & Chernyak, 2006a;b; Chertkov et al., 2020) techniques, as well as the combination of the two (Willisky et al., 2007).
- Our approach is also related to development of the MCMC techniques with polynomial guarantees, the so-called Fully Randomized Polynomial Schemes (FPRS), developed specifically for Ising models of a specialized, e.g. attractive (Jerrum & Sinclair, 1993) and zero-field, planar (Gómez et al., 2010; Ahn et al., 2016) types.

1.2. This Manuscript Contribution

We introduce fractional variational approximation interpolating between, by now classical, Tree Re-Weighted (TRW) and Belief Propagation (BP) cases. The fractional free energy, $\bar{F}^{(\lambda)} = -\log Z^{(\lambda)}$, defined as minus logarithm of the fractional approximation to the exact partition function, $Z = \exp(-\bar{F})$, requires solving an optimization problem, which is achieved practically by running a fractional version of one of the standard message-passing algorithm. Basic definitions, including problem formulation for the Ising models and variational formulation in terms of the node and edge beliefs (proxies for the respective exact marginal probabilities), are given in Section 2. Assuming that the fractional message-passing algorithm converges we study dependence of the Bethe Free energy on the fractional parameter, λ , and relation between the exact value of the free energy (minus logarithm of the exact partition function) and the fractional free energy. We report the following theoretical results:

- We show in Section 3 that $\bar{F}^{(\lambda)}$ is a continuous and monotone function of λ (Theorem 3.1 proved in Appendix B) which is also convex in λ (Theorem 3.2 proved in Appendix C).
- Our main theoretical result, Theorem 4.1, presented in Section 4 and proven in Appendix D, states that the exact partition function can be expressed as a product of the variational free energy and of the multiplicative correction, $Z = Z^{(\lambda)} \mathcal{Z}^{(\lambda)}$. The latter multiplicative correction term, $\mathcal{Z}^{(\lambda)}$, is stated as an explicit expectation of an expression over a well defined “mean-field” probability distribution, where both the expression and the “mean-field” probability distribution are stated explicitly in terms of the fractional node and edge beliefs.

The theory is extended with experiments reported in Section 5. Here we show, in addition to confirming our theoretical statements (and thus validating our simulation settings) that:

- Dependence of $\bar{F}^{(\lambda)}$ and $\log Z^{(\lambda)}$ on λ is of a phase transition type when we move from the TRW regime at $\lambda = 0$ to the BP regime at $\lambda > \bar{\lambda}$.
- Evaluating $Z^{(\lambda)} \mathcal{Z}^{(\lambda)}$ at different values of λ and confirming that the result is independent of λ suggests a novel approach to reliable and efficient estimate of the exact Z .
- Analyzing ensembles of the attractive Ising Models over graphs of size N we observe that fluctuations of the value of λ_* within the ensemble, where $Z^{(\lambda_*)} = Z$, decreases dramatically with increase in N . This observation suggest that estimating λ_* for an instance from the ensemble allows efficient approximate evaluation of Z for any other instances from the ensemble.
- Studying the sampling procedure to estimate $\mathcal{Z}^{(\lambda)}$, we observe that the number of samples required for the estimate is either independent on the system size, N , or possibly grows relatively weakly with N . This observation confirms that our approach to estimation of Z , consisting in evaluation of $Z^{(\lambda)}$ by a message-passing, then followed by drawing a small number of samples to estimate the correction, $\mathcal{Z}^{(\lambda)}$, is sound.
- Analysis of the mixed Ising ensembles (where attractive and repulsive edges alternate) suggests that for instances with sufficiently many repulsive edges finding, $\lambda_* \in [0, 1]$ may not be feasible.

We have a brief discussion of conclusions and path forward in Section 6.

2. Technical Preliminaries

2.1. Ising Models: the formulation

Graphical Models (GM) are the result of a marriage between probability theory and graph theory designed to express a class of high-dimensional probability distribution which factorize in terms of products of lower dimensional factors. The Ising model is an exemplary GM defined over an undirected graph, $\mathcal{G} = (\mathcal{V}, \mathcal{E})$. The Ising Model is stated in terms of binary variables, $x_a = \pm 1$, and singleton factors, $h_a \in \mathbb{R}$, associated with nodes of the graph, $a \in \mathcal{V}$ and pair-wise factors, $J_{ab} \in \mathbb{R}$, associated with edges of the graph, $(a, b) \in \mathcal{E}$. The probability distribution of the Ising

model observing a state, $\mathbf{x} = (x_a | a \in \mathcal{V})$ is

$$p(\mathbf{x} | \mathbf{J}, \mathbf{h}) = \frac{\exp(-E(\mathbf{x}; \mathbf{J}, \mathbf{h}))}{Z(\mathbf{J}, \mathbf{h})}, \quad (1)$$

$$Z(\mathbf{J}, \mathbf{h}) \doteq \sum_{\mathbf{x} \in \{\pm 1\}^{|\mathcal{V}|}} \exp(-E(\mathbf{x}; \mathbf{J}, \mathbf{h})), \quad (2)$$

$$E(\mathbf{x}; \mathbf{J}, \mathbf{h}) \doteq \sum_{(a,b) \in \mathcal{E}} E_{ab}(x_a, x_b), \quad (3)$$

$$\forall (a, b) \in \mathcal{E} : E_{ab} = -J_{ab}x_a x_b - (h_a x_a + h_b x_b)/2, \quad (4)$$

where $\mathbf{J} \doteq (J_{ab} | (a, b) \in \mathcal{E})$, $\mathbf{h} = (h_a | a \in \mathcal{V})$ are the pair-wise and singleton vectors, assumed given, $E(\mathbf{x}; \mathbf{J}, \mathbf{h})$ is the energy function and $Z(\mathbf{J}, \mathbf{h})$ is the partition function. Solving the Ising model inference problem means computing Z – which is, generally, requires efforts which are exponential in $N = |\mathcal{V}|$.

2.2. Exact Variational Formulation

Exact variational approach to computing Z consists in restating Eq. (2) in terms of the following Kullback-Leibler distance between $\exp(-E(\mathbf{x}; \mathbf{J}, \mathbf{h}))$ and a probe probability distribution, $\mathcal{B}(\mathbf{x}) \in [0, 1]^{|\mathcal{V}|}$, $\sum_{\mathbf{x}} \mathcal{B}(\mathbf{x}) = 1$, called belief:

$$\bar{F} = -\log Z = \min_{\mathcal{B}(\mathbf{x})} \sum_{\mathbf{x}} (E(\mathbf{x})\mathcal{B}(\mathbf{x}) - \mathcal{B}(\mathbf{x}) \log \mathcal{B}(\mathbf{x})), \quad (5)$$

where \bar{F} is also called (following widely accepted physics terminology) the free energy.

The exact variational formulation (5) is the starting point for approximate variational formulations, such as BP (Yedidia et al., 2005) and TRW (Wainwright & Jordan, 2007), stated solely in terms of the marginal beliefs associated with nodes and edges, respectively:

$$\forall a \in \mathcal{V}, \forall x_a : \mathcal{B}_a(x_a) \doteq \sum_{\mathbf{x} \setminus x_a} \mathcal{B}(\mathbf{x}), \quad (6)$$

$$\forall (a, b) \in \mathcal{E}, \forall x_a, x_b : \mathcal{B}_{ab}(x_a, x_b) \doteq \sum_{\mathbf{x} \setminus (x_a, x_b)} \mathcal{B}(\mathbf{x}). \quad (7)$$

Moreover, *fractional* approach developed in this manuscript provides variational formulation in terms of the marginal probabilities generalizing (and, in fact, interpolating between) respective BP and TRW approaches. Therefore, we now turn to stating the fractional variational formulation.

2.3. Fractional Variation Formulation

Let us introduce a fractional-, or λ -*reparametrization* of the belief (proxy for the probability distribution of \mathbf{x})

$$\mathcal{B}^{(\lambda)}(\mathbf{x}) = \frac{\prod_{\{a,b\} \in \mathcal{E}} (\mathcal{B}_{ab}(x_a, x_b))^{\rho_{ab}^{(\lambda)}}}{\prod_{a \in \mathcal{V}} (\mathcal{B}_a(x_a))^{\sum_{b \sim a} \rho_{ab}^{(\lambda)} - 1}}, \quad (8)$$

where $b \sim a$ is a shortcut notation for b such that, given $a \in \mathcal{V}$, $(a, b) \in \mathcal{E}$. Here in Eq. (8), $\rho_{ab}^{(\lambda)}$ is the λ -parameterized edge appearance probability

$$\rho_{ab}^{(\lambda)} = \rho_{ab} + \lambda(1 - \rho_{ab}), \quad \lambda \in [0, 1]. \quad (9)$$

which is expressed via the $\lambda = 0$ edge appearance probability, ρ_{ab} , dependent on the weighted set of the spanning trees, $\mathcal{T} \doteq \{T\}$, of the graph according to the following TRW rules (Wainwright & Jordan, 2007):

$$\forall (a, b) \in \mathcal{V} : \rho_{ab} = \sum_{T \in \mathcal{T}, \text{ s.t. } (a,b) \in T} \rho_T, \quad \sum_{T \in \mathcal{T}} \rho_T = 1. \quad (10)$$

A number of remarks are in order. First, $\lambda = 1$ corresponds to the case of BP. Then Eq. (8) is exact in the case of a tree graph, but it can also be considered as a (loopy) BP approximation in general. Second, and as mentioned above, $\lambda = 0$, corresponds to the case of TRW. Third, the newly introduced (joint) belief is not globally consistent, i.e. $\sum_{\mathbf{x}} \mathcal{B}^{(\lambda)}(\mathbf{x}) \neq 1$ for any λ , including the $\lambda = 0$ (TRW) and $\lambda = 1$ (BP) cases.

Substituting Eq. (8) into Eq. (5) we arrive at the following fractional approximation to the exact free energy stated as an optimization over all the node and edge marginal beliefs, $\mathcal{B} \doteq (\mathcal{B}_{ab}(x_a, x_b) | \forall \{a, b\} \in \mathcal{E}, x_a, x_b = \pm 1) \cup (\mathcal{B}_a(x_a) | \forall a \in \mathcal{V}, x_a = \pm 1)$

$$\bar{F}^{(\lambda)} \doteq \min_{\mathcal{B} \in \mathcal{D}} F^{(\lambda)}(\mathcal{B}), \quad F^{(\lambda)}(\mathcal{B}) \doteq E(\mathcal{B}) - H^{(\lambda)}(\mathcal{B}), \quad (11)$$

$$E(\mathcal{B}) \doteq \sum_{(a,b) \in \mathcal{E}} \sum_{x_a, x_b = \pm 1} E_{ab}(x_a, x_b) \mathcal{B}_{ab}(x_a, x_b), \quad (12)$$

$$H^{(\lambda)}(\mathcal{B}) \doteq - \sum_{(a,b) \in \mathcal{E}} \rho_{ab}^{(\lambda)} \sum_{x_a, x_b = \pm 1} \mathcal{B}_{ab}(x_a, x_b) \log \mathcal{B}_{ab}(x_a, x_b) + \sum_{a \in \mathcal{V}} \left(\sum_{b \sim a} \rho_{ab}^{(\lambda)} - 1 \right) \sum_{x_a = \pm 1} \mathcal{B}_a(x_a) \log \mathcal{B}_a(x_a), \quad (13)$$

$$\mathcal{D} \doteq \left\{ \mathcal{B} \left| \begin{array}{l} \mathcal{B}_a(x_a) = \sum_{x_b = \pm 1} \mathcal{B}_{ab}(x_a, x_b), \\ \forall a \in \mathcal{V}, \forall b \sim a, \forall x_a = \pm 1; \quad (a) \\ \sum_{x_a, x_b = \pm 1} \mathcal{B}_{ab}(x_a, x_b) = 1, \\ \forall (a, b) \in \mathcal{E}; \quad (b) \\ \mathcal{B}_{ab}(x_a, x_b) \geq 0, \\ \forall (a, b) \in \mathcal{E}, \forall x_a, x_b = \pm 1. \quad (c) \end{array} \right. \right\}. \quad (14)$$

The optimization over beliefs in Eq. (11) can be restated in the Lagrangian form (see Appendix A.1). Fixed points of the Lagrangian (potentially many) satisfy the so-called message-passing equations (see Appendix A.2). Then, the fractional free energy (partition function) is given, consistently with

all the formulas from the Appendices A.1,A.2, by

$$\begin{aligned}
Z^{(\lambda)} &= \exp\left(-\bar{F}^{(\lambda)}\right) = \exp\left(-F^{(\lambda)}(\mathcal{B}^{(\lambda)})\right) \quad (15) \\
&= \prod_{\{a,b\} \in \mathcal{E}} \left(\sum_{x_a, x_b} \exp\left(-\frac{E_{ab}(x_a, x_b)}{\rho_{ab}^{(\lambda)}}\right) \right) \times \\
&\quad \left(\mu_{b \rightarrow a}^{(\lambda)}(x_a) \right)^{\frac{\sum_a \rho_{ac}^{(\lambda)} - 1}{\rho_{ab}^{(\lambda)}}} \left(\mu_{a \rightarrow b}^{(\lambda)}(x_b) \right)^{\frac{\sum_b \rho_{bc}^{(\lambda)} - 1}{\rho_{ab}^{(\lambda)}}} \rho_{ab}^{(\lambda)} \times \\
&\quad \prod_{a \in \mathcal{V}} \left(\sum_{x_a} \prod_{b \sim a} \mu_{b \rightarrow a}^{(\lambda)}(x_a) \right)^{1 - \sum_a \rho_{ac}^{(\lambda)}}.
\end{aligned}$$

3. Properties of the Fractional Free Energy

Given construction of the fractional free energy, described above in Section 2.3 and also detailed in Appendix A, we are ready to make the following statements about the fractional free energy.

Theorem 3.1. [Monotonicity of the Fractional Free Energy] Assuming $\rho \doteq (\rho_{ab} | (a, b) \in \mathcal{E})$ is fixed, $\bar{F}^{(\lambda)}$ is a continuous, monotone function of λ .

Proof. See Appendix B. \square

Theorem 3.2. [Convexity of Fractional] Assuming $\rho \doteq (\rho_{ab} | (a, b) \in \mathcal{E})$ is fixed and the model is attractive, $\bar{F}^{(\lambda)}$ is a convex function of λ .

Proof. See Appendix C. \square

Notice that all the statements of this manuscript so far are made for an arbitrary Ising models, i.e. without any restrictions on the graph and vectors of the pair-wise interactions, \mathbf{J} and singleton biases, \mathbf{h} . It appears that if the discussion is limited to attractive (ferromagnetic) Ising models, $\forall (a, b) \in \mathcal{E} : J_{ab} \geq 0$, the following statement becomes a corollary of the Theorem 3.1

Lemma 3.3. [Exact Fractional] In the case of an attractive Ising model and any fixed ρ there exists $\lambda_* \in [0, 1]$ such that, $Z^{(\lambda_*)} = Z$.

Proof. Recall that by construction, $Z^{(\lambda=1)} \leq Z$, as proven in (Rozzi, 2012). In words, the partition function computed within the Bethe (BP) approximation results in a lower bound to the exact partition function. On the other hand, we know from (Wainwright & Jordan, 2007), and also by construction, that $Z^{(\lambda=0)} \geq Z$, i.e. TRW estimate of the partition function provides an upper bound to the exact partition function. These low and upper bounds, combined with the monotonicity of $Z^{(\lambda)}$ stated in Theorem 3.1 results in the desired statement. \square

4. Fractional Re-Parametrization for Exact Inference

Theorem 4.1. [Exact Relation Between Z and $Z^{(\lambda)}$]

$$Z = Z^{(\lambda)} \mathcal{Z}^{(\lambda)}, \quad (16)$$

$$\begin{aligned}
\mathcal{Z}^{(\lambda)} &\doteq \sum_{\mathbf{x}} \frac{\prod_{\{a,b\} \in \mathcal{E}} \left(\mathcal{B}_{ab}^{(\lambda)}(x_a, x_b) \right)^{\rho_{ab}^{(\lambda)}}}{\prod_{a \in \mathcal{V}} \left(\mathcal{B}_a^{(\lambda)}(x_a) \right)^{\sum_a \rho_{ac}^{(\lambda)} - 1}} \quad (17) \\
&= \mathbb{E}_{\mathbf{x} \sim p_0^{(\lambda)}(\cdot)} \left[\frac{\prod_{\{a,b\} \in \mathcal{E}} \left(\mathcal{B}_{ab}^{(\lambda)}(x_a, x_b) \right)^{\rho_{ab}^{(\lambda)}}}{\prod_{a \in \mathcal{V}} \left(\mathcal{B}_a^{(\lambda)}(x_a) \right)^{\sum_a \rho_{ac}^{(\lambda)}}} \right],
\end{aligned}$$

where the fractional BP expression for the partition function, $Z^{(\lambda)}$, is defined in Eq. (15); $p_0^{(\lambda)}(\mathbf{x}) \doteq \prod_a \mathcal{B}_a^{(\lambda)}(x_a)$ is the component-independent distribution devised from the FBP-optimal node-marginal probabilities.

Proof. See Appendix D \square

Notice that $\mathcal{Z}^{(\lambda)}$, defined in Eq. (17), is the exact multiplicative correction term, expressed in terms of the FBP solution, which should be equal to 1 at the optimal value of $\lambda^*(J, H)$, which is achievable, according to Lemma 3.3, in the case of the attractive Ising model.

5. Numerical Experiments

5.1. Setting, Use Cases and Methodology

In this Section we present results of our numerical experiments – supporting and also developing further theoretical results of the preceding Sections. Specifically, we will describe details of our experiments with the Ising model in the following “use cases”: (1) Over exemplary planar graph – $N \times N$ square grid, where $N = [3 :: 25]$; (2) Over a fully connected graph, K_N , where $N = [3 :: 8^2]$. In both cases we consider attractive models and mixed models – that is the models with some interactions being attractive (ferromagnetic), $J_{ab} > 0$, and some repulsive (antiferromagnetic), $J_{ab} < 0$. We experiment with the zero-field case, $\mathbf{h} = 0$, and also with the general (non-zero field) case. All of our models are “disordered” in the sense that we have generated samples of random \mathbf{J} and \mathbf{h} . Specifically, in the attractive (mixed) case components of \mathbf{J} are i.i.d. from the uniform distribution, $\mathcal{U}(0, 1)$ ($\mathcal{U}(-1, 1)$), and components of \mathbf{h} are i.i.d. from $\mathcal{U}(-1, 1)$. In some of our experiments we draw a single instance of \mathbf{J} and \mathbf{h} from the respective ensemble. However, in other experiments – aimed at analysis of the variability within the respective ensemble – we show results for a number of instances.

We know that there is a big freedom in selecting a set of spanning trees and then re-weighting respective contributions to $\rho \doteq (\rho_{ab} | (a, b) \in \mathcal{E})$ according to Eq. (10). (See some discussion of the experiments with possible ρ in (Wainwright et al., 2005)). However, we decided not to test the freedom, and instead, in all of our experiments ρ is chosen unambiguously for a given graph uniformly. As shown in (Wainwright, 2002), the edge-uniform re-weighting is optimal, i.e. it provides the lowest TRW upper-bound, in the case of highly symmetric graphs, such as fully connected or double-periodic square grid. It was also assumed in the TRW literature (but to the best of our knowledge never proven) that the edge-uniform re-weighting is (almost always) possible. We clarify this point in the following statement.

Lemma 5.1. (*[Edge-uniform Weights]*) *For any graph with all nodes of degree two or higher there exists a subset of spanning trees, such that each edge contributes at least one spanning tree, and the edge weight is calculated according to the edge-uniform rule: $\forall (a, b) \in \mathcal{V} : \rho_{ab} = (|\mathcal{V}| - 1)/|\mathcal{E}|$, where $|\mathcal{V}|$ is the number of vertices and $|\mathcal{E}|$ is the number of edges*¹.

Proof. See Appendix E for constructive proof. \square

To compute fractional free energy, $\bar{F}^{(\lambda)}$ (minus log of the fractional estimate for partition function), we generalize approach of (Bixler & Huang, 2018) which allows efficient, sparse-matrix based, implementation. Our code will be made available at github upon acceptance of the paper.

To compare the fractional estimate $\bar{F}^{(\lambda)} = -\log Z^{(\lambda)}$, with the exact free energy, $\bar{F} = -\log Z$, we either use direct computations (feasible for the 8×8 grid or smaller and for the fully connected graph over 64 nodes or smaller) or in the case of the planar grid and zero-field, when computation of the partition function is reduced to computing a determinant, we use the code from (Likhoshesterov et al., 2019) (see also references therein). Our computations are done for the values of λ equally spaced with the increment 0.05, between 0 and 1, $\lambda \in [0 :: 0.05 :: 1]$. We use Eq. (28) to estimate $d\bar{F}^{(\lambda)}/d\lambda$, and then use finite difference approximation for derivative and Eq. (29) to estimate $d^2\bar{F}^{(\lambda)}/d\lambda^2$.

The log-correction term, $\log \mathcal{Z}^{(\lambda)} = \log Z - \log Z^{(\lambda)}$, is estimated by direct sampling according to Eq. (17). (See Fig. (9) and respective discussion below for empirical analysis of the number of samples required to guarantee sufficient accuracy.)

¹The ‘‘degree two or higher’’ constraint on nodes is not restrictive, because we can either eliminate nodes with degree one (and also tree-like branches associated with them) by direct summation, or alternatively include the tree like branches in the appropriate number of spanning trees constructed for the graph ignoring the tree-like branches.

5.2. Properties of the Fractional Free Energy

Our numerical results for the fractional estimate of the log-partition function (minus fractional free energy), $\log Z^{(\lambda)} = -\bar{F}^{(\lambda)}$ and the log of the correction term, $\log \mathcal{Z}^{(\lambda)} = \log Z - \log Z^{(\lambda)} = \bar{F}^{(\lambda)} - \bar{F}$, are shown as functions of λ in Fig. (1) for the use cases described above². We draw from this set of Figures the following empirical conclusions:

- The monotonicity and convexity of $\bar{F}^{(\lambda)}$, proven in Theorem 3.1 and Theorem 3.2, respectively, are confirmed.
- Dependence of $\bar{F}^{(\lambda)}$ and $\log \mathcal{Z}^{(\lambda)}$ on λ is relatively sharp – of a phase transition type at some $\bar{\lambda}$, when we move from the TRW regime at $\lambda < \bar{\lambda}$ to the BP regime at $\lambda > \bar{\lambda}$. Notice that estimate of the threshold, $\bar{\lambda}$, decreases with the growth in N .

5.3. Relation between Exact and Fractional

Figs. (4,5, 6,7), shown in the Appendix F, also give an empirical confirmation to the Theorem 3.3 statement in the part which concerns independence of, $Z^{(\lambda)}\mathcal{Z}^{(\lambda)}$, of λ . This observation, combined with the full statement of the Theorem 3.3, suggests that if two or more of empirical estimates of $Z^{(\lambda)}\mathcal{Z}^{(\lambda)}$ at different λ are sufficiently close to each other we can use them to bound Z from above and below. Moreover, the full statement of the Theorem 4.1, i.e. equality between the left- and right- hand sides of Eq. (16), is also confirmed in all of our simulations with high accuracy (when we can verify it by computing Z directly).

5.4. Concentration of λ_* in Large Ensembles

Fig. (8) in the Appendix F shows dependence of $\bar{F}^{(\lambda)}$ on λ for a number of instances drawn from two exemplary attractive use-case ensembles. We observe that variability in the value of $\bar{F}^{(\lambda)}$ is sufficiently large. Variability of λ_* , where $Z^{(\lambda_*)} = Z$, are also observed, even though it is significantly smaller.

The last observation suggests that variability of λ_* within an attractive ensemble decreases with N when it grows. This guess is confirmed in our experiments with larger attractive ensembles illustrated in Fig. (2) for different N . For each N in the case over $N \times N$ grid we generate 4 different instances. We observe that as N increases variability of λ_* within the ensemble decreases dramatically. This observation is quite remarkable, as it suggests that it is enough to estimate λ_* for one instance in a large ensemble and then use it for accurate estimation of Z by simply computing $Z^{(\lambda_*)}$. Our estimations, based on the data shown in Fig. (2) and other similar experiments (not shown) suggest that the width of

²See also extended set of Figs. (4,5, 6,7) in the Appendix F, including dependence of $d\bar{F}^{(\lambda)}/d\lambda$, $d^2\bar{F}^{(\lambda)}/d\lambda^2$ on λ .

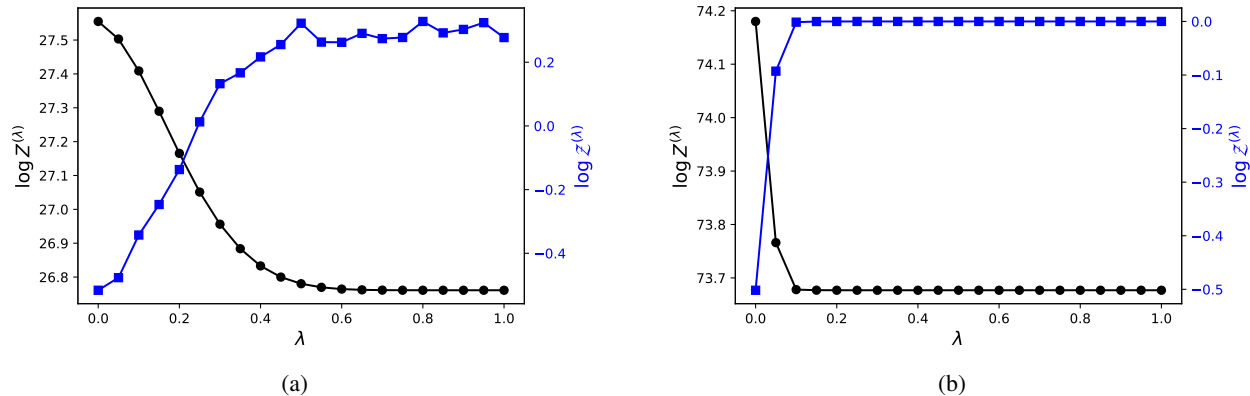


Figure 1. The case of the Ising Model (a) with non-zero field and random interaction, $h, J \sim \mathcal{U}(0, 1)$ over 3×3 planar grid; and (b) with non-zero field and random interaction, $h, J \sim \mathcal{U}(0, 1)$ over K_9 complete graph. We show fractional log-partition function (minus fractional free energy) - on the left- and the respective correction factor $\mathcal{Z}^{(\lambda)}$ - on the right vs the fractional parameter, λ .

the probability distribution of λ_* within the ensemble scales as $\propto 1/\sqrt{N}$ with increase in N .

5.5. Convergence of Sampling for $\mathcal{Z}^{(\lambda)}$

Fig. (9), shown in the Appendix F, reports dependence of the sample-based estimate of $\mathcal{Z}^{(\lambda)}$ on the number of samples. Our major observation here is that the result converges with the number of samples. Moreover, comparing the speed of convergence (with the number of samples) on the size of the system, N , we estimate that the latter scales with the former as $\mathcal{O}(N^{[2::4]})$.

5.6. Fractional Approach for Mixed (attractive and repulsive) Cases

Fig. (10) of the Appendix F, shows two distinct situations which may be observed in the mixed case where some of the interactions are attractive but other are repulsive, then allowing $Z^{(\lambda)}$ to be smaller or larger than Z . The former case is akin to the attractive model and $\lambda_* \in [0, 1]$, while in the later case there exists no $\lambda_* \in [0, 1]$ such that $Z^{(\lambda_*)} = Z$.

6. Conclusions and Path Forward

This manuscript suggests a new promising approach to evaluating inference in Ising Models. The approach consists in, first, solving a fractional variational problem via a distributed message-passing algorithm resulting in the fractional estimations for the partition function and marginal beliefs. We then compute multiplicative correction to the fractional partition function by evaluating a well-defined expectation of the mean-field probability distribution both constructed explicitly from the marginal beliefs. We showed that the freedom in the fractional parameter is useful, e.g.

for finding optimal value of the parameter, λ_* , where the multiplicative correction is unity. Our theory validated experiments result in a number of interesting observations, such as a phase-transition like dependence of the fractional free-energy on λ and strong suppression of fluctuations of λ_* in large ensembles.

As a path-forward we envision extending this fractional approach along the following directions:

- Proving or disproving the concentration conjecture and small number of samples conjecture, made informally in Section 5.4 and Section 5.5, respectively.
- Generalizing the extrapolation technique, e.g. building a scheme interpolating between TRW and Mean-Field. This will be of a special interest for the case of the mixed ensembles which are generally out of reach of the fractional approach (between TRW and BP) presented in the manuscript.
- Generalizing the extrapolation technique to more general class of Graphical Models.
- Extending the technique to the setting where λ_* will be learned directly from the data.

We also anticipate that all of these developments, presented in this manuscript and others to follow, will help to make variational GM techniques competitive with other, and admittedly more popular, methods of Machine Learning, such as Deep Learning (DL). We envision to see in the future more examples where the variational GM techniques will be re-enforced with the automatic differentiation, e.g. in the spirit of (Lucibello et al., 2022), and also integrated into modern Deep Learning protocols, e.g. as discussed in

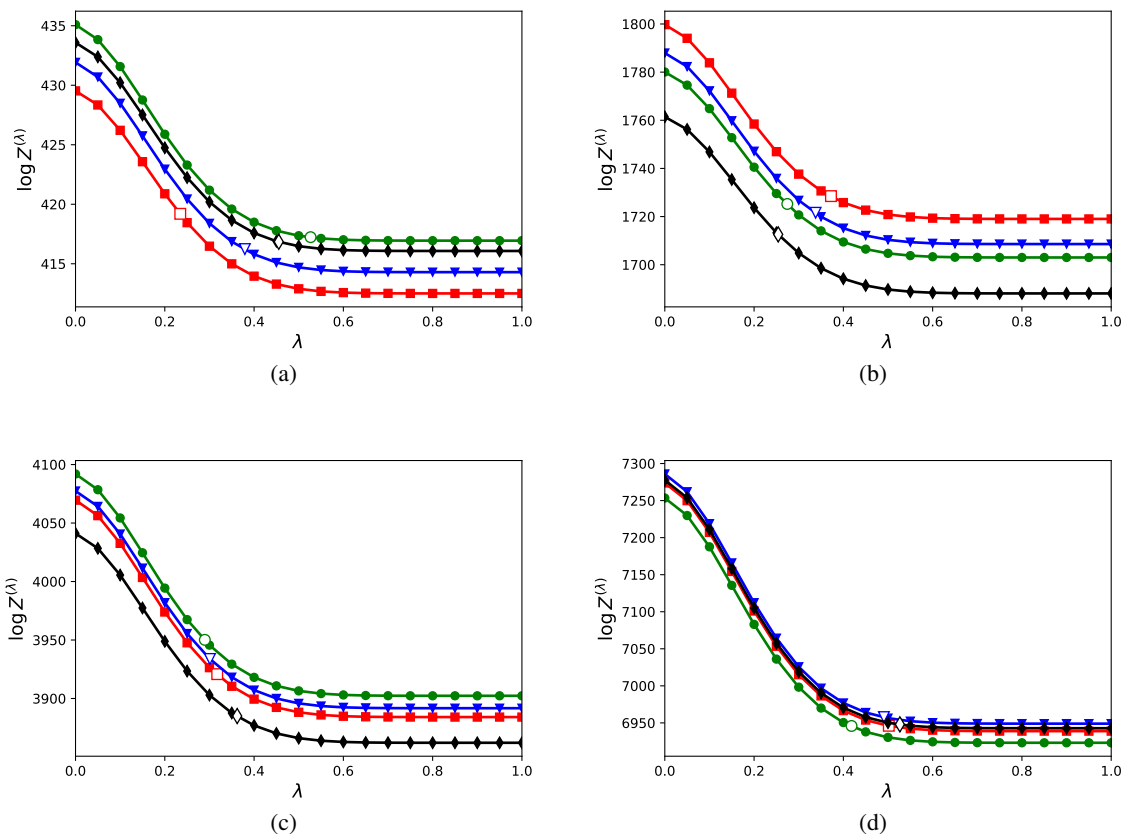


Figure 2. Planar zero-field Ising models for $n \times n$ grid with $J \sim \mathcal{U}(0, 1)$. For each n four different instances are generated by sampling uniformly at random from the unit interval and the exact values are shown by hollow marker on each graph. (a) 10×10 (b) 20×20 (c) 30×30 (d) 40×40 . Open symbols show respective values of λ_* .

(Garcia Satorras & Welling, 2021). This hybrid GM-DL approach is expected to be especially needed and powerful in the physics problems where we are interested to learn from data reduced models with graphical structure prescribed by the underlying physics (or other quantitative disciplines).

References

- Ahn, S., Chertkov, M., Weller, A., and Shin, J. Bucket Renormalization for Approximate Inference. volume 80 of *Proceedings of Machine Learning Research*, pp. 109–118. PMLR, Jul 2018.
- Ahn, S.-S., Chertkov, M., and Shin, J. Synthesis of MCMC and belief propagation. In *Advances in Neural Information Processing Systems*, volume 29. Curran Associates, Inc., 2016.
- Andrieu, C., de Freitas, N., Doucet, A., and Jordan, M. I. An introduction to MCMC for machine learning. *Machine Learning*, 50(1):5–43, Jan 2003.
- Bixler, R. and Huang, B. Sparse-Matrix Belief Propagation. In *Proceedings of the Conference on Uncertainty in Artificial Intelligence*, 2018.
- Chertkov, M. *INFERLO: Inference, Learning and Optimization with Graphical Models*. Leaving Book (self published for now), 2023. URL <https://t.ly/wkCR>.
- Chertkov, M. and Chernyak, V. Y. Loop calculus in statistical physics and information science. *Phys. Rev. E*, 73: 065102, Jun 2006a.
- Chertkov, M. and Chernyak, V. Y. Loop series for discrete statistical models on graphs. *Journal of Statistical Mechanics: Theory and Experiment*, 2006(06):P06009, Jun 2006b.
- Chertkov, M. and Yedidia, A. B. Approximating the permanent with fractional belief propagation. *Journal of Machine Learning Research*, 14(62):2029–2066, 2013.
- Chertkov, M., Chernyak, V., and Maximov, Y. Gauges, loops, and polynomials for partition functions of graphi-

- cal models. *Journal of Statistical Mechanics: Theory and Experiment*, 2020(12):124006, dec 2020.
- Dechter, R. Bucket elimination: A unifying framework for reasoning. *Artificial Intelligence*, 113(1):41–85, 1999.
- Dechter, R. and Rish, I. Mini-buckets: A general scheme for bounded inference. *J. ACM*, 50(2):107–153, Mar 2003. ISSN 0004-5411.
- Garcia Satorras, V. and Welling, M. Neural enhanced belief propagation on factor graphs. In Banerjee, A. and Fukumizu, K. (eds.), *Proceedings of The 24th International Conference on Artificial Intelligence and Statistics*, volume 130 of *Proceedings of Machine Learning Research*, pp. 685–693. PMLR, 13–15 Apr 2021.
- Gómez, V., Kappen, H. J., and Chertkov, M. Approximate inference on planar graphs using loop calculus and belief propagation. *Journal of Machine Learning Research*, 11(42):1273–1296, 2010.
- Jerrum, M. and Sinclair, A. Polynomial-time approximation algorithms for the ising model. *SIAM J. Comput.*, 22(5):1087–1116, oct 1993. ISSN 0097-5397.
- Likhoshervostov, V., Maximov, Y., and Chertkov, M. Inference and sampling of k_{33} -free ising models. In Chaudhuri, K. and Salakhutdinov, R. (eds.), *Proceedings of the 36th International Conference on Machine Learning*, volume 97 of *Proceedings of Machine Learning Research*, pp. 3963–3972. PMLR, 09–15 Jun 2019.
- Liu, Q. and Ihler, A. Bounding the partition function using hölder’s inequality. In *Proceedings of the 28th International Conference on International Conference on Machine Learning*, ICML’11, pp. 849–856, Madison, WI, USA, 2011. Omnipress. ISBN 9781450306195.
- Lucibello, C., Pittorino, F., Perugini, G., and Zecchina, R. Deep learning via message passing algorithms based on belief propagation. *Machine Learning: Science and Technology*, 3(3):035005, Jul 2022.
- Ruozzi, N. The bethe partition function of log-supermodular graphical models. In Pereira, F., Burges, C., Bottou, L., and Weinberger, K. (eds.), *Advances in Neural Information Processing Systems*, volume 25. Curran Associates, Inc., 2012.
- Wainwright, M., Jaakkola, T., and Willsky, A. A new class of upper bounds on the log partition function. *IEEE Transactions on Information Theory*, 51(7):2313–2335, 2005.
- Wainwright, M. J. *Stochastic processes on graphs with cycles: geometric and variational approaches*. phd, Massachusetts Institute of Technology, USA, 2002. AAI0804024.
- Wainwright, M. J. and Jordan, M. I. Graphical Models, Exponential Families, and Variational Inference. *Foundations and Trends® in Machine Learning*, 2007.
- Wainwright, M. J., Jaakkola, T., and Willsky, A. Tree-based reparameterization for approximate inference on loopy graphs. In *Advances in Neural Information Processing Systems*, volume 14. MIT Press, 2001.
- Wainwright, M. J., Jaakkola, T. S., and Willsky, A. S. Tree-reweighted belief propagation algorithms and approximate ML estimation by pseudo-moment matching. In *In AISTATS*, 2003.
- Welsh, D. The Computational Complexity of. Some Classical Problems from. Statistical Physics. In *Disorder in Physical Systems*, pp. 307–321. OxfordUniversityPress., 1991.
- Wiegerinck, W. and Heskes, T. Fractional Belief Propagation. In Becker, S., Thrun, S., and Obermayer, K. (eds.), *Advances in Neural Information Processing Systems*, volume 15. MIT Press, 2002.
- Willsky, A., Sudderth, E., and Wainwright, M. J. Loop series and bethe variational bounds in attractive graphical models. In Platt, J., Koller, D., Singer, Y., and Roweis, S. (eds.), *Advances in Neural Information Processing Systems*, volume 20. Curran Associates, Inc., 2007.
- Yedidia, J., Freeman, W., and Weiss, Y. Constructing Free-Energy Approximations and Generalized Belief Propagation Algorithms. *IEEE Transactions on Information Theory*, 51(7):2282–2312, 2005.
- Yedidia, J. S., Freeman, W. T., and Weiss, Y. Bethe free energy, Kikuchi approximations, and belief propagation algorithms. *Advances in neural information processing systems*, 13, 2001.

A. Fractional Variational Formulation: Details

A.1. Lagrangian formulation

Introducing Lagrangian multipliers associated with the linear constraints in Eqs. (14a,14b) we arrive at the following Lagrangian reformulation of Eq. (11)

$$\bar{F}^{(\lambda)} = \min_{\mathcal{B} \geq 0} \max_{\boldsymbol{\eta}, \boldsymbol{\psi}} L^{(\lambda)}(\mathcal{B}; \boldsymbol{\eta}, \boldsymbol{\psi}), \quad (18)$$

$$L^{(\lambda)} \doteq F^{(\lambda)}(\mathcal{B}) + \sum_{a \in \mathcal{V}; b \sim a} \sum_{x_a} \eta_{b \rightarrow a}(x_a) \left(\sum_{x_b} \mathcal{B}_{ab}(x_a, x_b) - \mathcal{B}_a(x_a) \right) + \sum_{\{a,b\} \in \mathcal{E}} \psi_{ab} \left(1 - \sum_{x_a, x_b} \mathcal{B}_{ab}(x_a, x_b) \right) \quad (19)$$

where $L^{(\lambda)}(\mathcal{B}; \boldsymbol{\eta}, \boldsymbol{\psi})$ is the (extended) Lagrangian dependent on both the primary variables (beliefs, \mathcal{B}) and the newly introduced dual variables, $\boldsymbol{\eta} \doteq (\eta_{b \rightarrow a}(x_a) \in \mathbb{R} | \forall a \in \mathcal{V}, \forall b \sim a, \forall x_a = \pm 1)$ and $\boldsymbol{\psi} \doteq (\psi_{ab} \in \mathbb{R} | \forall a \in \mathcal{V})$. Stationary point of the Lagrangian (19), assuming that it is unique, is defined by the following system of equations

$$\forall \{a, b\} \in \mathcal{E}, \forall x_a, x_b = \pm 1: \quad \frac{\delta L^{(\lambda)}(\mathcal{B})}{\delta \mathcal{B}_{ab}(x_a, x_b)} = 0 \Rightarrow \quad (20)$$

$$E_{ab}(x_a, x_b) + \rho_{ab}^{(\lambda)} \left(\log \left(\mathcal{B}_{ab}^{(\lambda)}(x_a, x_b) \right) + 1 \right) - \psi_{ab}^{(\lambda)} + \eta_{b \rightarrow a}^{(\lambda)}(x_a) + \eta_{a \rightarrow b}^{(\lambda)}(x_b) = 0,$$

$$\forall a \in \mathcal{V}, \forall x_a = \pm 1: \quad \frac{\delta L^{(\lambda)}(\mathcal{B})}{\delta \mathcal{B}_a(x_a)} = 0 \Rightarrow \left(\sum_{b \sim a} \rho_{ab}^{(\lambda)} - 1 \right) \left(\log \mathcal{B}_a^{(\lambda)}(x_a) + 1 \right) + \sum_{b \sim a} \eta_{b \rightarrow a}^{(\lambda)}(x_a) = 0, \quad (21)$$

augmented with Eqs. (14a,14b). Eqs. (20) and Eqs. (21) results in the following expressions for the marginals in terms of the Lagrangian multipliers

$$\forall a \in \mathcal{V}, \forall x_a = \pm 1: \quad \mathcal{B}_a^{(\lambda)}(x_a) \propto \exp \left(- \frac{\sum_{b \sim a} \eta_{b \rightarrow a}^{(\lambda)}(x_a)}{\sum_{b \sim a} \rho_{ab}^{(\lambda)} - 1} \right), \quad (22)$$

$$\forall \{a, b\} \in \mathcal{E}, \forall x_a, x_b = \pm 1: \quad \mathcal{B}_{ab}^{(\lambda)}(x_a, x_b) \propto \exp \left(- \frac{E_{ab}(x_a, x_b) + \eta_{b \rightarrow a}^{(\lambda)}(x_a) + \eta_{a \rightarrow b}^{(\lambda)}(x_b)}{\rho_{ab}^{(\lambda)}} \right). \quad (23)$$

Here in Eqs. (20,21,22,23) and below the upper index (λ) in $\mathcal{B}^{(\lambda)}, \eta^{(\lambda)}$ and $\psi^{(\lambda)}$ variables indicates that the respective variables are optimal, i.e. argmax and argmin, over respective optimizations in Eq. (19).

A.2. Message Passing

We may also rewrite Eqs. (22,23) in terms of the so-called message (from node-to-node) variables. Then the marginal beliefs are expressed via the $\mu^{(\lambda)}$ -messages according to

$$\forall a \in \mathcal{V}, \forall b \sim a: \quad \mu_{b \rightarrow a}^{(\lambda)}(x_a) \doteq \exp \left(- \frac{\eta_{b \rightarrow a}^{(\lambda)}(x_a)}{\sum_{b \sim a} \rho_{ab}^{(\lambda)} - 1} \right), \quad (24)$$

$$\forall a \in \mathcal{V}, \forall x_a = \pm 1: \quad \mathcal{B}_a^{(\lambda)}(x_a) = \frac{\prod_{b \sim a} \mu_{b \rightarrow a}^{(\lambda)}(x_a)}{\sum_{x_a} \prod_{b \sim a} \mu_{b \rightarrow a}^{(\lambda)}(x_a)}, \quad (25)$$

$$\forall \{a, b\} \in \mathcal{E}, \forall x_a, x_b = \pm 1: \quad \mathcal{B}_{ab}^{(\lambda)}(x_a, x_b) = \frac{\exp \left(- \frac{E_{ab}(x_a, x_b)}{\rho_{ab}^{(\lambda)}} \right) \left(\mu_{b \rightarrow a}^{(\lambda)}(x_a) \right)^{\frac{\sum_{c \sim a} \rho_{ac}^{(\lambda)} - 1}{\rho_{ab}^{(\lambda)}}} \left(\mu_{a \rightarrow b}^{(\lambda)}(x_b) \right)^{\frac{\sum_{c \sim b} \rho_{bc}^{(\lambda)} - 1}{\rho_{ab}^{(\lambda)}}}}{\sum_{x_a, x_b} \exp \left(- \frac{E_{ab}(x_a, x_b)}{\rho_{ab}^{(\lambda)}} \right) \left(\mu_{b \rightarrow a}^{(\lambda)}(x_a) \right)^{\frac{\sum_{c \sim a} \rho_{ac}^{(\lambda)} - 1}{\rho_{ab}^{(\lambda)}}} \left(\mu_{a \rightarrow b}^{(\lambda)}(x_b) \right)^{\frac{\sum_{c \sim b} \rho_{bc}^{(\lambda)} - 1}{\rho_{ab}^{(\lambda)}}}}, \quad (26)$$

and the Fractional Belief Propagation (FBP) equations, expressing relations between pairwise and singleton marginals become:

$$\forall a \in \mathcal{V}, \forall b \sim a, \forall x_a = \pm 1 : \quad (27)$$

$$\mathcal{B}_a^{(\lambda)}(x_a) \propto \prod_{b \sim a} \mu_{b \rightarrow a}^{(\lambda)}(x_a) \propto \sum_{x_b} \exp\left(-\frac{E_{ab}(x_a, x_b)}{\rho_{ab}^{(\lambda)}}\right) \left(\mu_{b \rightarrow a}^{(\lambda)}(x_a)\right)^{\frac{\sum_{c \sim a} \rho_{ac}^{(\lambda)} - 1}{\rho_{ab}^{(\lambda)}}} \left(\mu_{a \rightarrow b}^{(\lambda)}(x_b)\right)^{\frac{\sum_{c \sim b} \rho_{bc}^{(\lambda)} - 1}{\rho_{ab}^{(\lambda)}}} \propto \sum_{x_b} \mathcal{B}_{ab}^{(\lambda)}(x_a, x_b).$$

Note (on a tangent), that the $\mu^{(\lambda)}$ -(message) variables introduced here are related but not equivalent to the $M^{(\lambda)}$ -messages which can also be seen used in the BP-literature, see e.g. Section 4.1.3 of (Wainwright & Jordan, 2007). Specifically in the case of BP, i.e. when $\rho_{ab}^{(\lambda)} = 1$, relation between $\mu^{(\lambda)}$ and $M^{(\lambda)}$ variables is as follows, $(\mu_{b \rightarrow a}^{(\lambda)}(x_a))^{d_a - 1} = \prod_{c \sim a; c \neq b} M_{c \rightarrow a}^{(\lambda)}(x_a)$.

B. Proof of Theorem 3.1

Let us evaluate derivative of the fractional free energy (11) over λ explicitly

$$\begin{aligned} \frac{d}{d\lambda} \bar{F}^{(\lambda)} &= \frac{d}{d\lambda} F^{(\lambda)}(\mathcal{B}^{(\lambda)}) = \sum_{\{a,b\}} \sum_{x_a, x_b} \frac{\partial F^{(\lambda)}(\mathcal{B}^{(\lambda)})}{\partial \mathcal{B}_{ab}^{(\lambda)}(x_a, x_b)} \frac{d\mathcal{B}_{ab}^{(\lambda)}(x_a, x_b)}{d\lambda} + \sum_a \sum_{x_a} \frac{\partial F^{(\lambda)}(\mathcal{B}^{(\lambda)})}{\partial \mathcal{B}_a^{(\lambda)}(x_a)} \frac{d\mathcal{B}_a^{(\lambda)}(x_a)}{d\lambda} \\ &\quad - \sum_{\{a,b\}} \frac{\partial H^{(\lambda)}(\mathcal{B}^{(\lambda)})}{\partial \rho_{ab}^{(\lambda)}} \frac{d\rho_{ab}^{(\lambda)}}{d\lambda}. \end{aligned}$$

Taking into account for the conditions of stationarity of the fractional free energy, tracking explicit dependencies of the fractional entropy on $\rho_{ab}^{(\lambda)}$, and thus on λ , we arrive at

$$\begin{aligned} \forall \{a, b\} : \quad \frac{\partial F^{(\lambda)}(\mathcal{B}^{(\lambda)})}{\partial \mathcal{B}_{ab}^{(\lambda)}(x_a, x_b)} &= 0; \quad \forall a : \quad \frac{\partial F^{(\lambda)}(\mathcal{B}^{(\lambda)})}{\partial \mathcal{B}_a^{(\lambda)}(x_a)} = 0; \\ \frac{\partial H^{(\lambda)}(\mathcal{B}^{(\lambda)})}{\partial \rho_{ab}^{(\lambda)}} &= - \sum_{x_a, x_b = \pm 1} \mathcal{B}_{ab}^{(\lambda)}(x_a, x_b) \log \mathcal{B}_{ab}^{(\lambda)}(x_a, x_b) + \sum_{x_a = \pm 1} \mathcal{B}_a^{(\lambda)}(x_a) \log \mathcal{B}_a^{(\lambda)}(x_a) + \sum_{x_b = \pm 1} \mathcal{B}_b^{(\lambda)}(x_b) \log \mathcal{B}_b^{(\lambda)}(x_b) \\ &= -I_{ab}^{(\lambda)}, \end{aligned}$$

where the newly introduced $I_{ab}^{(\lambda)}$ is nothing but the pairwise mutual information defined according to $\mathcal{B}^{(\lambda)}$. Notice that $I_{ab}^{(\lambda)} \geq 0$. Since, $d\rho_{ab}^{(\lambda)}/d\lambda = 1 - \rho_{ab} \geq 0$, and summarizing all of the above we derive

$$\frac{d}{d\lambda} \bar{F}^{(\lambda)} = - \sum_{\{a,b\}} (1 - \rho_{ab}) I_{ab}^{(\lambda)} \leq 0, \quad (28)$$

therefore concluding proof of both continuity (the derivative is bounded) and monotonicity (the derivative is negative).

C. Proof of Theorem 3.2

Let us express the second derivative of the fractional free energy over λ explicitly using Eq. (28),

$$\frac{d^2}{d\lambda^2} \bar{F}^{(\lambda)} = - \sum_{\{a,b\}} (1 - \rho_{ab}) \frac{d}{d\lambda} I_{ab}^{(\lambda)}. \quad (29)$$

To show that the second derivative is positive (convexity claim), it is sufficient to prove the following lemma.

Lemma C.1. Assuming $\rho \doteq (\rho_{ab} | (a, b) \in \mathcal{E})$ is fixed, $I_{ab}^{(\lambda)}$ is monotone decreasing in λ .

Proof. Consider, first, the case of the Ising model in zero field, where the minimum of the fractional free energy is achieved at a highly symmetric beliefs

$$\forall a \in \mathcal{V} : \mathcal{B}_a(x_a) = 1/2, \quad \forall (a, b) \in \mathcal{E} : \mathcal{B}_{ab}(x_a, x_b) = \begin{pmatrix} \beta_{ab}^{(\lambda)} & 1/2 - \beta_{ab}^{(\lambda)} \\ 1/2 - \beta_{ab}^{(\lambda)} & \beta_{ab}^{(\lambda)} \end{pmatrix}.$$

It allows the following simplification of the mutual information in terms of the marginal beliefs

$$\begin{aligned} I_{ab}^{(\lambda)}(x_a, x_b) &= \sum_{x_a, x_b = \pm 1} \mathcal{B}_{ab}^{(\lambda)}(x_a, x_b) \log \mathcal{B}_{ab}^{(\lambda)}(x_a, x_b) - \sum_{x_a = \pm 1} \mathcal{B}_a^{(\lambda)}(x_a) \log \mathcal{B}_a^{(\lambda)}(x_a) - \sum_{x_b = \pm 1} \mathcal{B}_b^{(\lambda)}(x_b) \log \mathcal{B}_b^{(\lambda)}(x_b) \\ &= 2 \left(\beta_{ab}^{(\lambda)} \log \beta_{ab}^{(\lambda)} + (1/2 - \beta_{ab}^{(\lambda)}) \log(1/2 - \beta_{ab}^{(\lambda)}) \right) + \log 2 + \log 2 \\ &= 2 \left(\beta_{ab}^{(\lambda)} \log \beta_{ab}^{(\lambda)} + (1/2 - \beta_{ab}^{(\lambda)}) \log(1/2 - \beta_{ab}^{(\lambda)}) + 1 \right). \end{aligned}$$

Then evaluating derivative of the mutual information over λ we arrive at

$$\frac{dI_{ab}^{(\lambda)}}{d\lambda} = \frac{dI_{ab}^{(\lambda)}}{d\beta_{ab}^{(\lambda)}} \frac{d\beta_{ab}^{(\lambda)}}{d\lambda} = \log \left(\frac{\beta_{ab}^{(\lambda)}}{1/2 - \beta_{ab}^{(\lambda)}} \right)^2 \frac{d\beta_{ab}^{(\lambda)}}{d\lambda} \leq 0,$$

The first term in the expression is always positive because,

$$1/4 = \mathcal{B}_a \mathcal{B}_b < \beta_{ab}^{(\lambda)} < \min\{\mathcal{B}_a, \mathcal{B}_b\} = 1/2,$$

where $\beta_{ab}^{(\lambda)}$ is a decreasing function of λ (since the model is attractive).

To extend this derivation to the general case of $\mathbf{h} \neq 0$ we follow the (standard) transformation from the general Ising model to its zero-field equivalent by introducing an extra node connected to all other nodes:

$$p(\mathbf{x}) \propto \exp \left(\sum_{a \in \mathcal{V}} h_a x_a + \sum_{(a,b) \in \mathcal{E}} J_{ab} x_a x_b \right) \propto p(\mathbf{x}, x_*) \propto \exp \left(\sum_{a \in \mathcal{V}} J_{a*} x_a x_* + \sum_{(a,b) \in \mathcal{E}} J_{ab} x_a x_b \right),$$

where x_* is the newly introduced node connected to all original nodes and $J_{a*} = h_*$. It is easy to see that $Z(\mathbf{J}, \mathbf{h}) = Z^*(\mathbf{J}^*, \mathbf{0})/2$ where Z^* is the partition function on the modified graph with new interaction \mathbf{J}^* . □

D. Proof of Theorem 4.1

Consistently with Eq. (8), Eqs. (25,26) allow us to rewrite the joint probability distribution in terms of the optimal beliefs which solve the fractional Eqs. (27)

$$\begin{aligned} p(\mathbf{x}) &= Z^{-1} \prod_{\{a,b\} \in \mathcal{E}} \left(\sum_{x_a, x_b} \exp \left(-\frac{E_{ab}(x_a, x_b)}{\rho_{ab}^{(\lambda)}} \right) \left(\mu_{b \rightarrow a}^{(\lambda)}(x_a) \right)^{\frac{\sum_{c \sim a} \rho_{ac}^{(\lambda)} - 1}{\rho_{ab}^{(\lambda)}}} \left(\mu_{a \rightarrow b}^{(\lambda)}(x_b) \right)^{\frac{\sum_{c \sim b} \rho_{bc}^{(\lambda)} - 1}{\rho_{ab}^{(\lambda)}}} \right)^{\rho_{ab}^{(\lambda)}} \times \\ &\prod_{a \in \mathcal{V}} \left(\sum_{x_a} \prod_{b \sim a} \mu_{b \rightarrow a}^{(\lambda)}(x_a) \right)^{\sum_{c \sim a} \rho_{ac}^{(\lambda)} - 1} \frac{\prod_{\{a,b\} \in \mathcal{E}} \left(\mathcal{B}_{ab}^{(\lambda)}(x_a, x_b) \right)^{\rho_{ab}^{(\lambda)}}}{\prod_{a \in \mathcal{V}} \left(\mathcal{B}_a^{(\lambda)}(x_a) \right)^{\sum_{c \sim a} \rho_{ac}^{(\lambda)} - 1}}. \end{aligned} \quad (30)$$

Normalization condition, that is the requirement for the sum on the right hand side of Eq. (30) to return 1, results in the desired statement, i.e. Eqs. (16,17).

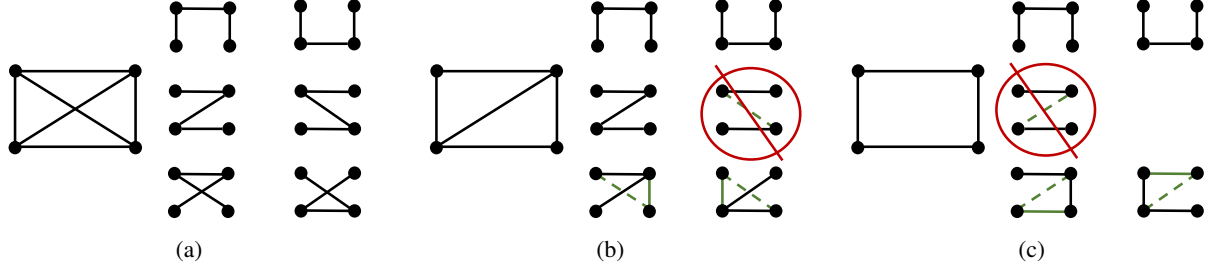


Figure 3. Construction of the set of spanning trees for a sequence of graphs built from the K_4 graph (sub-figure (a)) in two steps, from (a) to (b) and from (b) to (c), each time eliminating an edge. At each step we remove one edge (shown dashed green), remove one spanning tree (shown circled and crossed red), and add a new edge (shown solid green) to all the remaining spanning trees which lost an edge such that they stay spanning trees and the resulting ρ_{ab} edges are uniform among the remaining spanning trees. The resulting number of spanning trees and the uni-form edge weights are (a) $|\mathcal{V}| = 4$ and $\forall(a, b) \in \mathcal{V}$, $\rho_{ab} = |\mathcal{V}| - 1/|\mathcal{E}| = (4 - 1)/6 = 3/6 = 1/2$; (b) $|\mathcal{V}| = 5$ and $\forall(a, b) \in \mathcal{V}$, $|\mathcal{V}| - 1/|\mathcal{E}| = (4 - 1)/5 = 3/5$; (c) $|\mathcal{V}| = 4$ and $\forall(a, b) \in \mathcal{V}$, $|\mathcal{V}| - 1/|\mathcal{E}| = (4 - 1)/4 = 3/4$.

Algorithm 1 Edge-Uniform Set of Spanning Trees

Input: K_N , graph. Sequence of edges, $\{e_1, \dots, e_{N-2}\}$ of K_N and respective sequence of graphs, $\{\mathcal{G}_1, \dots, \mathcal{G}_{N-2}\}$, such that, $\mathcal{G}_1 = K_N \setminus e_1, \forall n = 1, \dots, N - 3 : \mathcal{G}_{n+1} \doteq \mathcal{G}_n \setminus e_{n+1}$, and \mathcal{G}_{N-2} is a single loop

Initialize: \mathcal{T} - set of all linear spanning trees of \mathcal{G} . (A spanning tree is linear if all nodes is of degree two or one.)

Repeat: $n = 1, \dots$

1. $\mathcal{G} = (\mathcal{V}, \mathcal{E}) = \mathcal{G}_n$
2. $\forall T \in \mathcal{T} : \rho_T = 1/|\mathcal{E}|$ and thus $\forall(a, b) \in \mathcal{E} : \rho_{ab} = (|\mathcal{V}| - 1)/|\mathcal{E}|$.
3. Exit if $n = N - 2$.
4. Remove edge e_n from all spanning trees in \mathcal{T}
5. $\mathcal{T} \leftarrow \mathcal{T} \setminus$ (element of \mathcal{T} which becomes disconnected)
6. Modify \mathcal{T} by adding an extra edge to each spanning tree of \mathcal{T} having $(N - n - 1)$ edges. These added edges should keep each element of \mathcal{T} a spanning tree of \mathcal{G} and also guarantee that each edge enters exactly $N - 1$ resulting spanning trees. (It is straightforward to check that such a construction is unique and unambiguous. See Fig. (3) for illustration.)

E. Proof of Lemma 5.1

Our proof of the statement is constructive and it is thus formalized in the Algorithm 1. The Algorithm follows induction, starting from a complete graph and then progressing by removing edges (and therefore loops) sequentially, such that at any step all nodes continue to be of degree two or larger. The induction terminates when the resulting graph is a single loop. See Fig. (3) for illustration on the example of $N = 4$, thus K_4 .

The proof allows to construct the required set of spanning trees for any graph (with all nodes of degree two or larger) because by selecting a sequence of edges in the Algorithm 1 proper we can arrive at the given graph starting from the complete graph containing as many nodes as the given graph and eliminating edges according to the Algorithm 1.

F. More Figures from Numerical Experiments

We show in this Appendix an extended set of Figures for the experiments discussed in the Section 5.3 of the main text. Specifically, results of our experiment for the case of the Ising model over planar graphs and complete graphs of various sizes in the settings of zero- and non-zero- fields are illustrated in Figs. (4,5, 6,7). We show in this set of figures dependence of $\log Z^{(\lambda)} = -\bar{F}^{(\lambda)}$ and $\log \mathcal{Z}^{(\lambda)}$, as well as $d\bar{F}^{(\lambda)}/d\lambda$ and $d^2\bar{F}^{(\lambda)}/d\lambda^2$, on λ . Observing dependence of the first and second derivatives of the fractional free energy on λ allows us to conclude (confirm) that the log fractional partition function

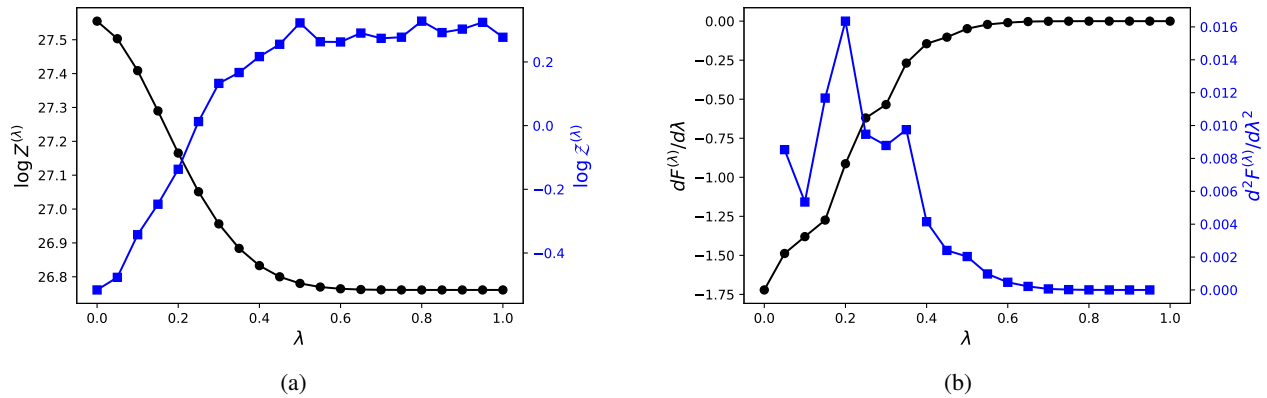


Figure 4. The case of the Ising Model with non-zero magnetic field and random interaction, $h, J \sim \mathcal{U}(0, 1)$ over 3×3 planar grid. We show (a) fractional log-partition function (minus fractional free energy) - on the left- and the respective correction factor $\mathcal{Z}^{(\lambda)}$ - on the right vs the fractional parameter, λ ; (b) the first order derivative - on the left - and second order derivative - on the right - vs λ .

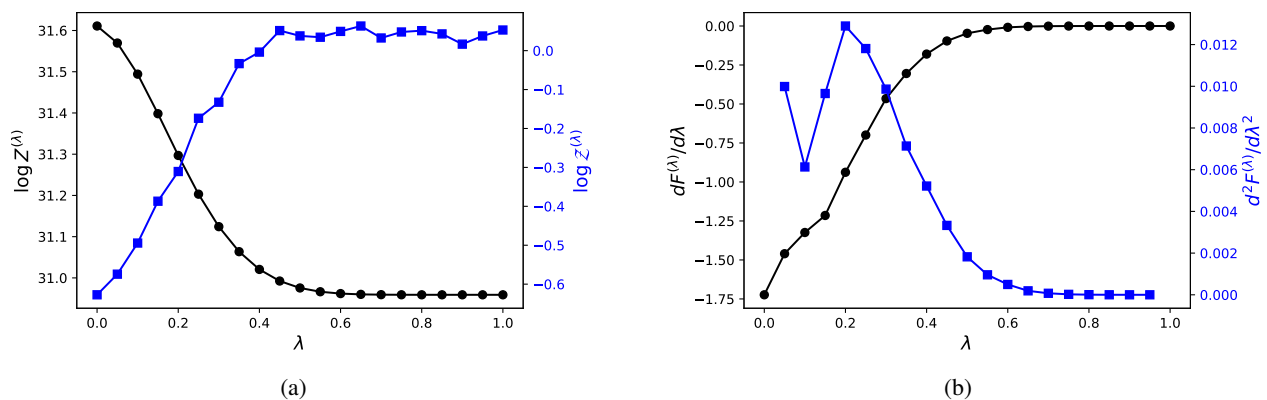


Figure 5. The case of the Ising Model with zero magnetic field and random interaction, $J \sim \mathcal{U}(0, 1)$ over 3×3 planar grid. Further details are identical to used in Fig. (4).

is monotone decreasing and also convex in λ . We also observe that when λ is sufficiently large, $\log Z^{(\lambda)}$ is independent of λ . We also track in these figures the value of λ_* , correspondent to $\mathcal{Z}^{(\lambda_*)} = 1$, and thus $Z = Z^{(\lambda_*)}$.

Fig. (8), mentioned in Section 5.4 shows λ_* for a number of instances drawn from the respective ensembles of the Ising model (over planar and complete graphs). We observe that in the planar case, $\lambda_* \in [0.25, 0.45]$, while in the case of the complete graph, $\lambda_* \in [0.05, 0.15]$.

Fig. (9), mentioned in Section 5.5, shows results for the experiments with the Ising model of two different sizes. We see here estimation of the correction factor, $\log Z^{(\lambda)}$, evaluated at different λ for a varying number of samples (drawn i.i.d. from the mean-field distribution built based of the fractional nodal beliefs). We observe that the estimate stops to change with increase in the number of samples, once a sufficient number of samples, M_c , is drawn. We estimate that M_c grows with N as $\mathcal{O}(N^4)$ or slower.

Fig. (10), mentioned in Section 5.6, shows results for the mix case when the pair-wise interaction can vary in sign from edge to edge. In this mixed case, as seen in the presented examples, we can not guarantee that BP provides a lower bound on the partition function, and thus λ_* may or may not be identified within the $[0, 1]$ interval.

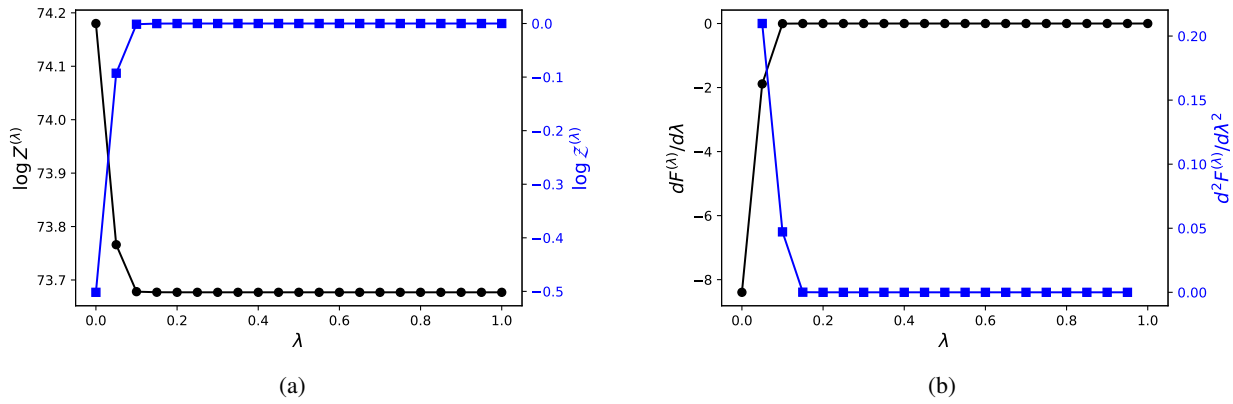


Figure 6. The case of the Ising Model with non-zero magnetic field and random interaction, $h, J \sim \mathcal{U}(0, 1)$ over K_9 complete graph. Further details are identical to used in Fig. (4).

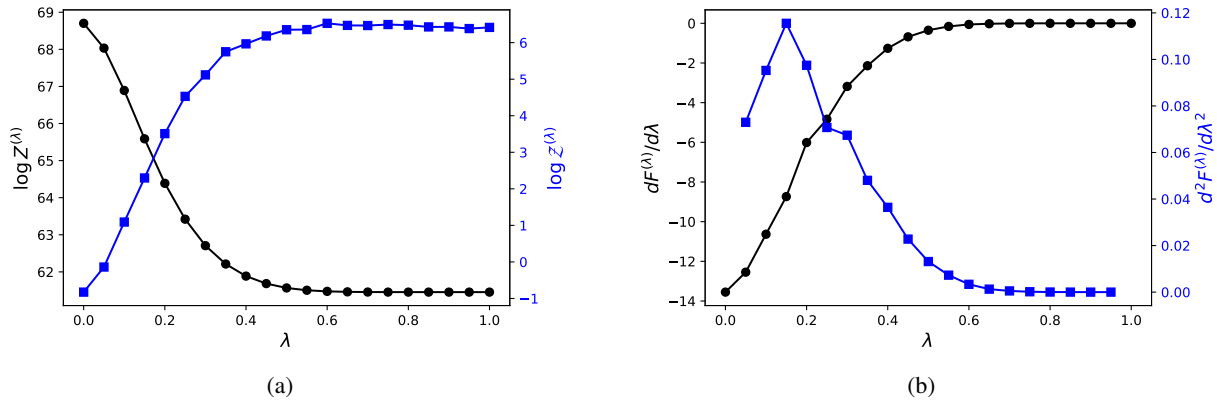


Figure 7. The case of the Ising Model with zero magnetic field and random interaction, $J \sim \mathcal{U}(0, 1)$ over K_9 complete graph. Further details are identical to used in Fig. (4).

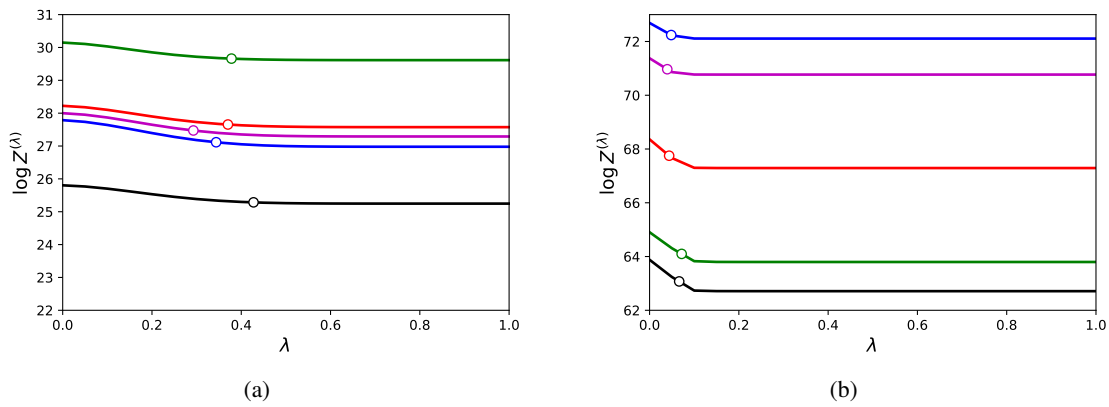


Figure 8. $F^{(\lambda)}$ vs λ for a number of instances (shown in different colors) drawn for the Ising model ensembles over, (a) 3×3 grid, and (b) K_9 graph, where elements of \mathbf{J} and \mathbf{h} are i.i.d. from $\mathcal{U}(0, 1)$. Circles mark respective exact values, λ_* .

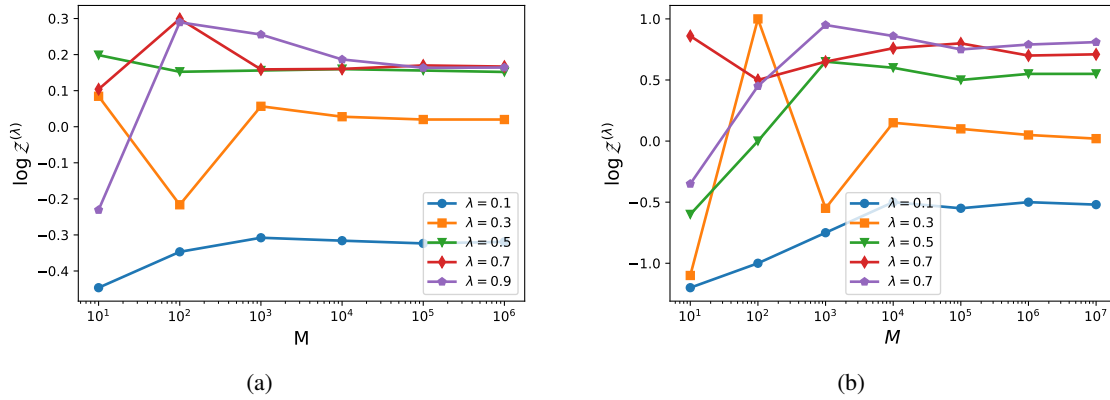


Figure 9. Dependence of the sample-based estimate of $Z^{(\lambda)}$ on the number of samples in the case of attractive Ising model over (a) 3×3 , and (b) 6×6 grids, where elements of J and h are drawn i.i.d. from $\mathcal{U}[0, 1]$. Different colors correspond to different values of λ .

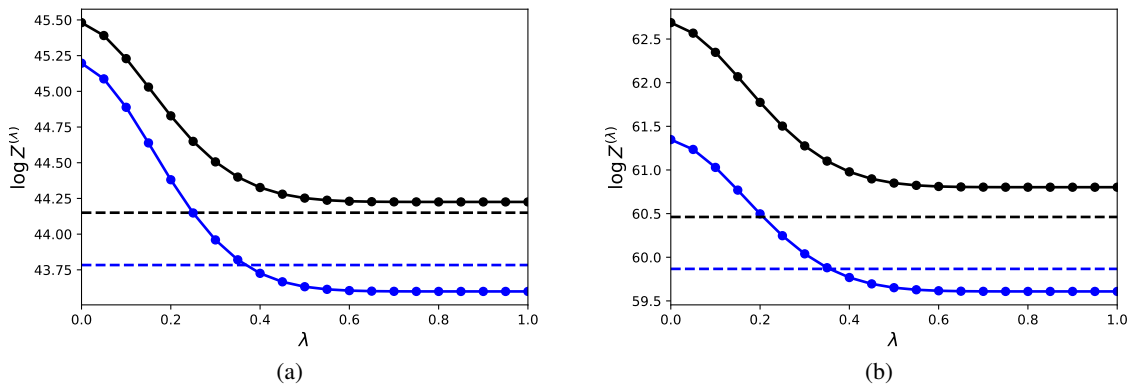


Figure 10. Two different random instance of 4×4 Ising Model with (a) $J \sim \mathcal{U}(-1, 1)$ and $h \sim \mathcal{U}(-1, 1)$ (b) $J \sim \mathcal{U}(-1, 1)$, $h = 0$. Dashed line show exact value of partition functions for the corresponding curve.